Journal of Physics: Conference Series **298** (2011) 012022 doi:10.1088/1742-6596/298/1/012022

Compton transmission polarimeter for a very precise polarization measurement within a wide range of electron currents

R Barday[1], K Aulenbacher[2], P Bangert[1], J Enders[1], A Göök[1], D H Jakubassa-Amundsen[3], F Nillius[2], A Surzhykov[4] and V A Yerokhin[5]

[1] Institut für Kernphysik, TU Darmstadt, Schlossgartenstr. 9, 64289 Darmstadt, Germany
[2] Institut für Kernphysik, Universität Mainz, J. J. Becherweg 45, 55118 Mainz, Germany
[3] Mathematisches Institut, Universität München, Theresienstr. 39, 80333 München, Germany
[4] Physikalisches Institut, Universität Heidelberg, Philosophenweg 12, 69120 Heidelberg, Germany
[5] Center for Advanced Studies, St. Petersburg State Polytechnical University, Polytekhnicheskaya 29, 195251 St. Petersburg, Russia

E-mail: barday@ikp.tu-darmstadt.de

Abstract. For new experiments with polarized electron and positron beams the precise and quick measurement of the beam polarization is required. The relative electron polarization has been monitored on-line using a compact transmission Compton polarimeter for a wide range of average electron currents up to 100 μA and electron beam energy of 3.5 MeV. The asymmetry induced by the beam polarization can be monitored precisely with $\Delta A/A < 0.2\,\%$. Even small relative variations of the beam polarization during a beam time may be detected using this polarimeter, such as an increase $\sim 1\,\%$ and subsequent decrease of the beam polarization.

1. Introduction

Different methods based on Mott and Møller scattering can be applied for polarization measurement. These polarimeters are destructive and cannot be operated during an experimental run. One has to assume that the polarization remains constant during the data taking or interrupt the experiment repeatedly for a polarization measurement. "Standard" Mott polarimeters are suitable up to electron beam energies of several MeV and are sensitive to the transverse beam polarization only. "Standard" Møller polarimeters are suitable at higher beam energies, but at low currents only (few μA), because of target heating. Another method is to analyse the circular polarization of the bremsstrahlung radiation produced when the electron beam hits a target. A simple way to measure the circular polarization of the photons is by determining their transmission through a magnetized absorber. Here one exploits the polarization dependence of the Compton scattering cross section: The transmitted intensity of circularly polarized photons scattered from the longitudinally polarized electrons in the magnetized absorber depends on the relative orientation of the photon and the electron spins. By switching the helicity of the photon beam, an asymmetry can be calculated.

2. Polarization transfer in bremsstrahlung

Circularly polarized bremsstrahlung radiation is produced when a polarized electron beam hits a radiator target. We will restrict ourselves to longitudinally polarized electrons, since for transversely polarized electrons the polarization transfer efficiency is smaller. This transfer efficiency depends on the energy E_γ and the emission angle θ of the photon. In the ultrarelativistic limit where the photons are nearly exclusively emitted in forward direction, Olsen and Maximon [1] have, based on approximate (Sommerfeld-Maue) electronic wavefunctions, derived the following expression for the circular polarization P_γ

$$P_\gamma = \frac{E_\gamma}{E_i} \frac{1 + \frac{1}{3}\left(1 - \frac{E_\gamma}{E_i}\right)}{1 - \frac{2}{3}\left(1 - \frac{E_\gamma}{E_i}\right) + \left(1 - \frac{E_\gamma}{E_i}\right)^2} P_e, \tag{1}$$

where $E_i = E_e + mc^2$ is the total energy of the electron beam and P_e is the polarization of the electron beam. Numerical calculations within the Elwert-Haug theory (for $E_\gamma < E_e$) performed at $E_e = 2 - 20\,\mathrm{MeV}$ and $\theta = 1°$ show that equation (1) performs quite well (figure 1). In the short wavelength limit, $E_\gamma = E_e$, the polarization transfer is nearly complete at $E_e \geq 2\,\mathrm{MeV}$. From the Born approximation for bremsstrahlung, McVoy [2] has derived the following formula for circular polarization at the short wavelength limit and $\theta = 0°$

$$P_\gamma{}^{max} = \left(1 + \frac{(1-\beta)\,(E_e + 2mc^2)}{(2-\beta)\,E_e}\right)^{-1} P_e, \tag{2}$$

which is plotted in figure 2 as a function of E_e. Also shown are numerical results from a more elaborate theory which uses Sommerfeld-Maue functions for the fast electron and Dirac functions for the slow one [3] at $E_e \geq 0.5$ MeV, respectively from partial wave calculations [4] at $E_e \leq 3$ MeV. Clearly, P_γ/P_e drops rapidly at beam energies below 1 MeV. We recall that neither of the formulae (1) or (2) depends on the nuclear charge Z of the radiator target. This Z-independence is, however, no longer true for low energies and when θ becomes large.

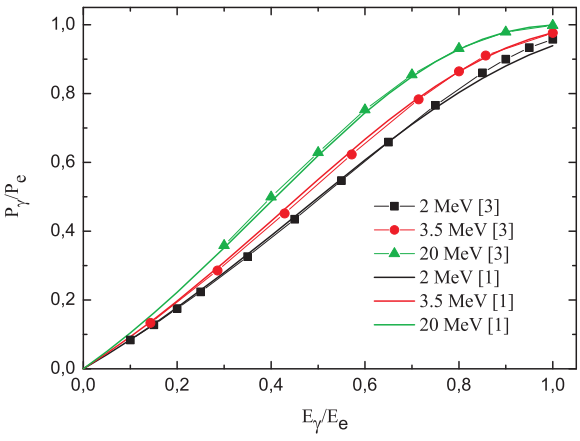

Figure 1. Circular polarization of bremsstrahlung radiation created by longitudinally polarized electron beam on Cu.

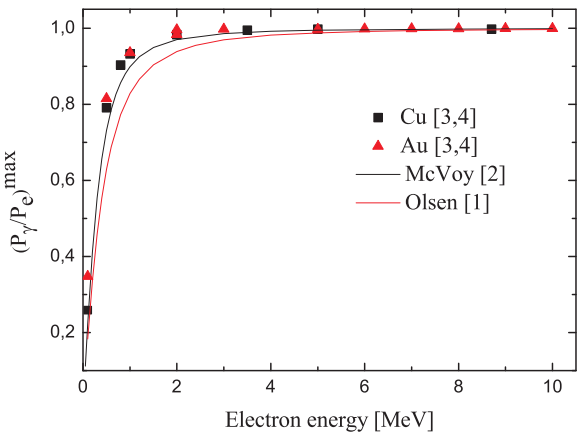

Figure 2. Efficiency of the polarization transfer as a function of the electron beam energy at the short wavelength limit.

3. Polarized Compton scattering

The Compton scattering of the photons with circular polarization P_γ from polarized electrons is given by [5]

$$\frac{d\sigma_c}{d\Omega} = \frac{r_0^2}{2}\left(\frac{k}{k_0}\right)^2 \{\phi_0 + fP_\gamma\phi_3\} \tag{3}$$

with $\phi_0 = 1 + \cos^2\theta + (k_0 - k)(1 - \cos\theta)$ and $\phi_3 = -(1 - \cos\theta)(k_0 + k)\cos\theta$. Here, r_0 is the classical electron radius, k_0 is the initial and k is the final photon momentum after scattering, ϕ_0 gives the ordinary Compton cross section, ϕ_3 is the polarization-dependent Compton cross section, θ is the scattering angle, and f is the fraction of longitudinally polarized electrons in the absorption magnet. By integrating the differential cross section, one obtains the total scattering cross section in the form

$$\sigma_c = \sigma_c^0 + fP_\gamma\sigma_c^{pol}, \tag{4}$$

where σ_c^0 is the polarization-insensitive (Klein-Nishina) and

$$\sigma_c^{pol} = \pm 2\pi r_0^2 \left\{\frac{1}{k_0} + \frac{k_0}{(1+2k_0)^2} - \frac{(1+k_0)}{2k_0^2}\ln(1+2k_0)\right\} \tag{5}$$

is the polarization-sensitive part. The term in the brackets changes sign at a photon energy of about 0.64 MeV and is negative at $E_\gamma > 0.64$ MeV. The photon transmission depends on the relative orientation of the photon and electron spins. The positive sign in equation (5) corresponds to the photon spin parallel to the electron spin and hence antiparallel to the magnetization. Or, in other words, for photon energies $E_\gamma > 0.64$ MeV the transmission is higher when the photon spin is parallel to the electron spin. The efficiency of the Compton transmission polarimeter depends on the ratio $|Z\sigma_c^{pol}/\sigma_{tot}|$, which has a maximum at 5 MeV (figure 3). Hence the measurement of the beam polarization using a Compton transmission polarimeter is most effective for energies of several MeV. At higher energies, for example at $E_e = 1.508$ GeV [6], the analyzing power of the Compton transmission polarimeter is very low, which makes an accurate polarization measurement challenging.

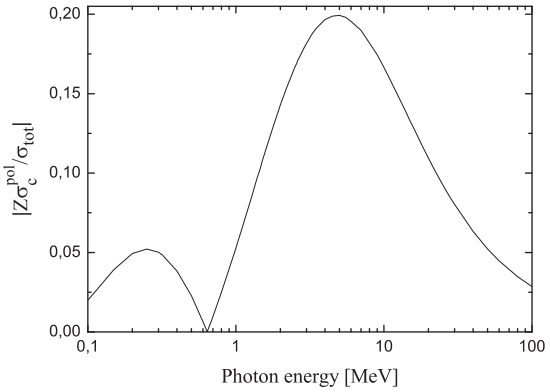

Figure 3. Ratio of the polarization dependent Compton cross section to the total cross section as a function of the photon energy for VACOFLUX50.

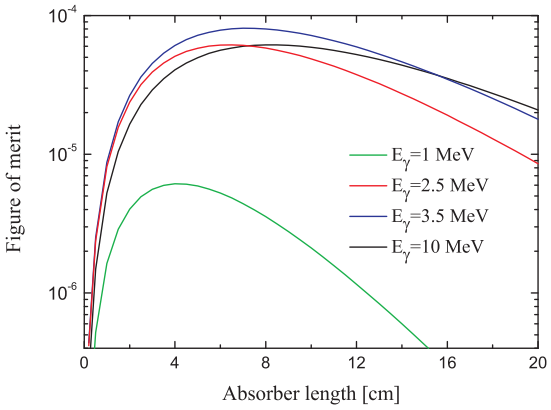

Figure 4. Dependence of the figure of merit on the length of the absorber for different photon energies.

The transmission probability for photons through the magnetized absorber of length L is given by

$$T^{\pm} = \exp\{-nL\sigma_{tot}\} = \exp\{-nL(\sigma_{photo} + \sigma_{pair} + Z\sigma_c)\}, \tag{6}$$

where n denotes the number density of atoms in the absorber. The asymmetry is then given by

$$A = \frac{T^+ - T^-}{T^+ + T^-} = \tanh\left(-nLZfP_\gamma\sigma_c^{pol}\right) \sim \left(-nLZfP_\gamma\sigma_c^{pol}\right), \tag{7}$$

because $nLZfP_\gamma\sigma_c^{pol} < 0.1$. The asymmetry in transmission increases linearly with increasing length of the absorber, but the intensity passing the absorber falls exponentially. If the counting rate is the limiting factor for the accuracy of the measurement, the optimum length $L_{opt} = 2\,(n\sigma_{total})^{-1}$ may be found from minimizing $\Delta A/A$, where ΔA is the statistical error in the asymmetry A and σ_{total} is the total absorption cross section. A figure of merit for the polarimeter A^2T for different photon energies as a function of the length of the absorption magnet is plotted in figure 4. Calculations are done using a photon polarization of 80 % and an electron polarization in the absorber of $f = 8$ %. If the counting rate is large, the length of the absorber can be increased to enhance the asymmetry. The absorber of the polarimeter described below consists of a 9 cm core and return yokes. The asymmetry of the transmitted intensity calculated using equation (7) for a 9 cm absorption magnet and the results from figure 1 for P_γ are shown in figure 5 as a function of the photon energy.

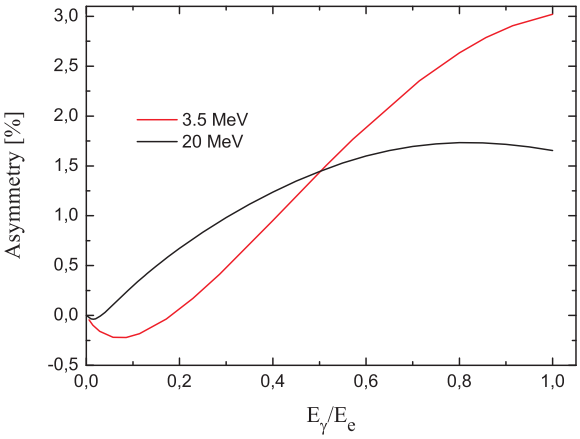

Figure 5. Predicted asymmetry as a function of the photon energy for the incident electron beam energies of 3.5 and 20 MeV.

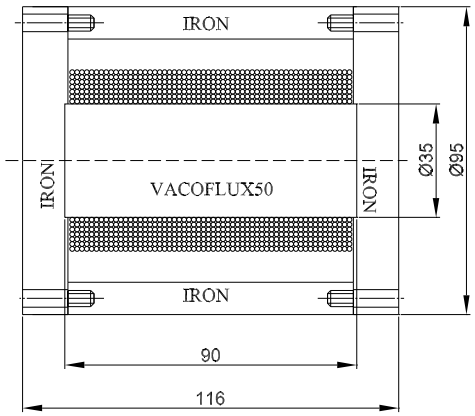

Figure 6. The absorption magnet with 420 turns, symbolized by the rows of circles.

4. Polarimeter

The Compton transmission polarimeter consists of a radiator, which produces the bremsstrahlung radiation, two CsI(Tl) detectors to measure the intensity of the photons and a magnetized absorber. As a radiator target we have chosen a copper target with a length of 12 mm. Our simulation shows that not more than 0.04 % of the incident electrons penetrate through the radiator. The electron polarization in the magnetized absorber is determined by

$$f = \frac{M_s}{N_e\mu_B} \sim \frac{2M}{N_e\mu_B}\left(\frac{g'-1}{g'}\right), \tag{8}$$

where M_s is the magnetization due to electron spin, M is the total magnetization, N_e is the electron density, μ_B is the Bohr magneton, and g' is the magnetomechanical ratio. The core of the absorption magnet is made from VACOFLUX50 (49%Co, 1.9%V and 49.1%Fe). VACOFLUX50 has a Curie temperature of 1223 K and an electron polarization of 8.5% at

2.35 T. High magnetization is achieved through annealing in a dry hydrogen atmosphere at 820^0C. The dimensions and shape of the absorption magnet are shown in figure 6. The ends of the core are machined with high precession to be flat and perpendicular to the axis.
Because of the photomultipliers saturation at high electron currents and high operation voltage, we use a silicon PIN photodiode (SPD) to read out the scintillation light. A combination of a scintillator with a SPD has a number of advantages for the photon detection, like high detection efficiency, high light output, temperature dependence of the signal only in the crystal part, insensitivity to magnetic fields and compactness. To read out the scintillation light of CsI(Tl), with a peak emission wavelength at 550 nm a Hamamatsu S3204 PIN-photodiode with an active area of $18\times18\,\mathrm{mm}^2$ is used. The quantum efficiency of the SPD at 550 nm is about 80 %. The CsI(Tl) scintillator was purchased from Saint-Gobain and has dimensions of $17\times17\,\mathrm{mm}^2$ and 50 mm length. After polishing all faces of the scintillator, it was wrapped in Teflon, followed by aluminium foil. The optical connection between the photodiode and the crystal is a RTV based silicon glue manufactured by GE Bayer Silicones. The energy resolution of the detector is about 6 % FWHM for 1332 keV.

5. Polarization measurements

The experiment has been performed at the MAMI injector [7]. A polarized electron beam is produced by illuminating a $GaAs/GaAs_{0.64}P_{0.36}$ strained superlattice photocathode [8] with circularly polarized light of 776 nm. The electron beam is accelerated to 3.5 MeV and deflected to 30^0 by the dipole magnet for the polarization measurement, as is shown in figure 7.

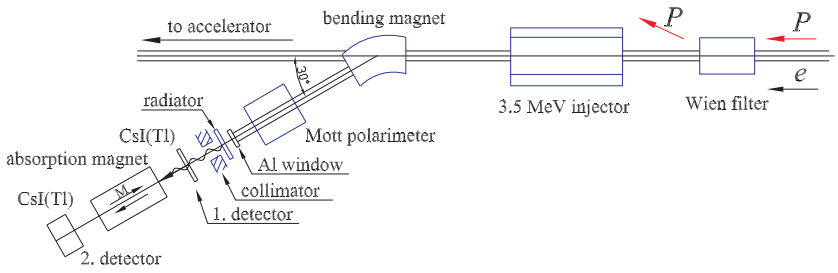

Figure 7. Layout of the experimental area.

The asymmetry of the transmitted photons determined in the experiment is given by

$$A = \frac{I_2^+/I_1^+ - I_2^-/I_1^-}{I_2^+/I_1^+ + I_2^-/I_1^-}, \tag{9}$$

where $I_1^\pm$ and $I_2^\pm$ are the signals from the first and second detector for two different helicities of the beam, respectively. We measured the dependence of the asymmetry on the current $I_{absorber}$ in the absorption magnet (figure 8). The electron beam current was 8 μA, and the electron spins were oriented at 45^0 with respect to the beam direction using the Wien filter to control the beam polarization using a Mott polarimeter additionally. Each measurement took about 60 seconds. One recognizes the hysteresis effects. About 1100 Ampere turns are needed to saturate the absorber. To limit heating of the absorption magnet it was magnetized in the later experiments using a current of 2.8 A.

The dependence of the asymmetry on the average electron beam current was also investigated. The polarization vector was, again, oriented at 45^0 with respect to the beam orientation. The transmission between the gun and the polarimeter in this experiment was approximately 90 %. We observed a slight change of the asymmetry of about $\Delta A/A \sim 10^{-4}$ (figure 9(a)) per μA

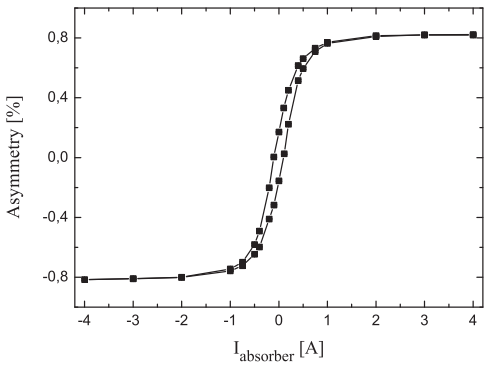

Figure 8. "Hysteresis loop" measured with polarized electron beam.

of beam current. This could be an effect of the thermal heating of the photocathode. The cathode holder is not optimized with respect to the heat transfer. Most of the laser intensity will be transferred to the crystal lattice of the photocathode, causing a temperature increase. This might affect the beam polarization. To see how temperature affects the spin polarization, consider the polarization dependence on the relaxation time

$$P = \frac{P_0}{1 + \tau/\tau_s} B_{BBR}, \tag{10}$$

where P_0 is the initial electron polarization in the conduction band, τ is the photoemission time of electrons, τ_s is the spin relaxation time, and B_{BBR} represents the depolarization in the band-bending region. The photoemission time τ amounts to several picoseconds and is approximately temperature independent, but τ_s decreases with increasing temperature [9]. Hence it can be expected that the polarization decreases at higher currents.

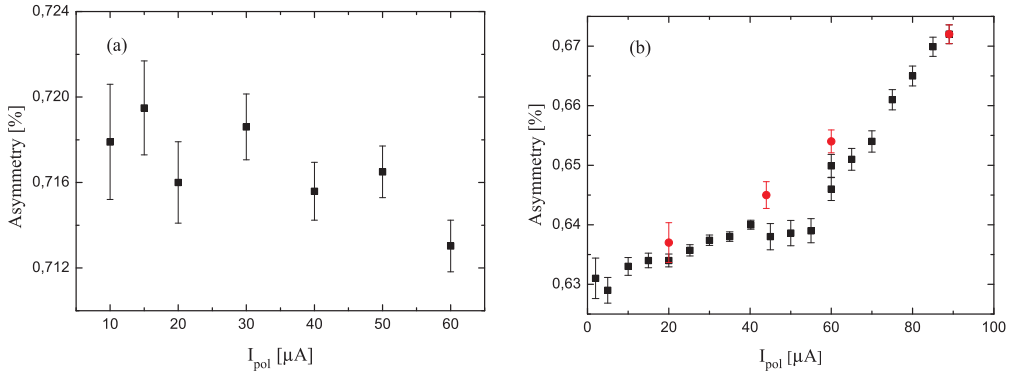

Figure 9. Observations of Compton asymmetry vs beam current I_{pol} at polarimeter. Black datapoints in left and right figures are subsequent measurements with an interruption of three months in between them. I_{pol} variation for the black points was obtained by varying the laser intensity on the cathode, the 'red' dataset in the right figure was obtained by reducing the beam current, produced by a constant laser intensity, by a variable electron beam collimator slit.

Three months later we repeated the experiment. The first detector was irradiated with gamma rays with about 10 kGy. The change of the asymmetry for currents below 60 μA is of the same order as three months ago, but has an opposite sign, perhaps because of the radiation damage.

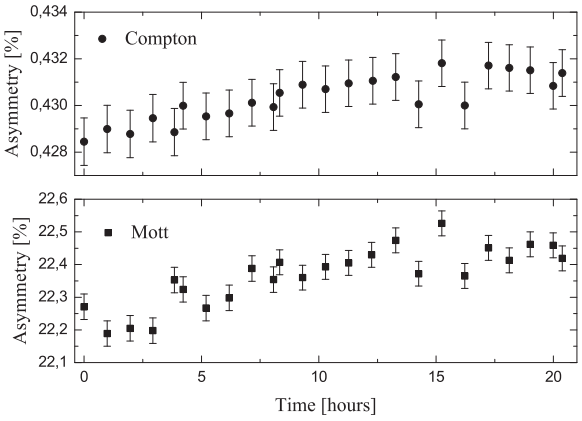

Figure 10. Variation of the electron spin polarization during a beam time, measured with Compton and Mott polarimeter.

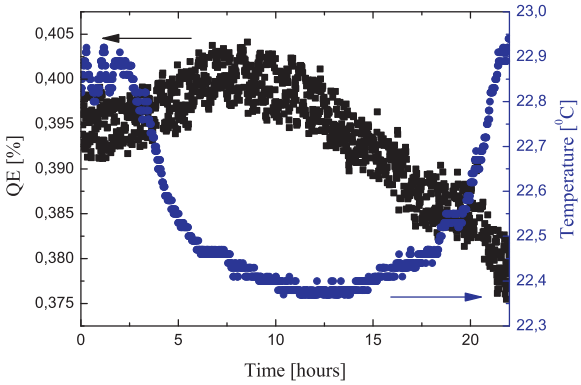

Figure 11. Quantum efficiency (squares) and temperature (circles) near the gun.

At higher beam currents the change of the asymmetry is significantly greater. The non-linearity of the photon detectors is responsible for this effect. To show that the change of the asymmetry in figure 9(b) is not an effect of the photocathode, we increased the laser power to produce $100\,\mu A$ average current from the gun and kept it constant. The beam current I_{pol} delivered to the polarimeter was reduced with a movable collimator slit in the chopper system between the source and the first accelerating structure. For both types of variation the current dependence is very similar, which provides strong evidence that the variation is not caused by intensity dependent effects - such as cathode heating - in the photocathode.

The long-term variation of the electron spin polarization was studied, as well. Data taking started 23 hours after cathode activation. The electron beam current delivered to the polarimeter was $30\,\mu$A, the polarization angle was 45^0. In order to make the Compton and Mott measurements simultaneously, we moved a 250-nm-thick gold target into the Mott polarimeter. Both polarimeters show an approximately linear increase of the polarization 15 hours after the start of the measurement (figure 10). During this experiment the quantum efficiency of the photocathode and the temperature near the gun were monitored (figure 11). The maximum polarization was observed 7 hours after the maximum of the quantum efficiency at a QE of $\sim 97\%$ of the maximum value. A similar behaviour of the polarization was observed in [10].

Acknowledgments

The authors want to thank C. Weinrich for helpful discussion. This work was supported by the Deutsche Forschungsgemeinschaft through SFB 443 and SFB 634 and by the state of Hesse through the LOEWE centre HIC for FAIR.

References

[1] Olsen H and Maximon L C 1959 *Phys. Rev.* **114** 887
[2] McVoy K W 1957 *Phys. Rev.* **106** 828 (Erratum: 1958 *Phys. Rev.* **110** 1484)
[3] Jakubassa-Amundsen D H 2010 *Phys. Rev.* A **82** 042714
[4] Yerokhin V A and Surzhykov A, submitted to publication
[5] Schopper H 1958 *Nucl. Instr.* **3** 158
[6] Weinrich C private communication and 2005 *Eur. Phys. J.* A **24** s2 129
[7] Aulenbacher K 1997 *Nucl. Instr. and Meth.* A **391** 498
[8] Maruyama T 2005 Proc. 16th Int. Spin Symp. SPIN2004 (Singapore: World Scientific) 917
[9] Kurebayashi H 2010 *Appl. Phys. Lett.* **96** 022505 and Zerrouati K 1988 *Phys. Rev.* B **37** 1334
[10] Mamaev Yu A 2001 AIP Conf. Proc. vol 570 p 920 and Tawada M 1997 *Jpn. J. Appl. Phys.* **36** 2863.